Author(s): Hakonen, Pertti J. & Vuorinen, R. T. & Martikainen, J. E.

Title: Nuclear antiferromagnetism in rhodium metal at positive and negative nanokelvin temperatures

Year: 1993

Version: Final published version

Please cite the original version:

Hakonen, Pertti J. & Vuorinen, R. T. & Martikainen, J. E. 1993. Nuclear antiferromagnetism in rhodium metal at positive and negative nanokelvin temperatures. Physical Review Letters. Volume 70, Issue 18. 2818-2821. ISSN 0031-9007 (printed). DOI: 10.1103/physrevlett.70.2818

Nuclear Antiferromagnetism in Rhodium Metal at Positive and Negative Nanokelvin Temperatures

P. J. Hakonen, R. T. Vuorinen, and J. E. Martikainen
Low Temperature Laboratory, Helsinki University of Technology, 02150 Espoo, Finland
(Received 1 February 1993)

We have measured the dynamic susceptibility of polycrystalline rhodium foils down to 280 pK and up to -750 pK. These record-low and -high nuclear spin temperatures were reached by adiabatic demagnetization using initial polarizations of 83% and -60%. At $T>0$, the static susceptibility, integrated from NMR spectra, displays an antiferromagnetic Curie-Weiss law, with $\theta=-1.8\pm0.3$ nK. At $T<0$, a crossover from ferro- to antiferromagnetic tendency is found around -6 nK. We obtain $J_{nn}/h=-17\pm3$ Hz and $J_{nnn}/h=10\pm3$ Hz if only nearest and next nearest neighbor interactions are assumed.

PACS numbers: 75.30.Kz, 75.90.+w

Nuclear magnetism in metals has been investigated extensively at ultralow temperatures during the past few years [1]. Recently, it was shown that nuclear magnetic ordering in silver can be studied even at negative absolute spin temperatures, and that in this metal antiferromagnetism at $T>0$ transforms into ferromagnetism at $T<0$ [2]. Rhodium provides another nuclear spin system in which negative temperatures can be produced. In Rh there is close competition between isotropic and anisotropic nuclear interactions, which leads to interesting structures when $T<0$.

At negative spin temperatures, a nuclear system tries to organize itself so that the Helmholtz free energy is maximized in zero field [3]. In a system dominated by antiferromagnetic nearest neighbor exchange interactions, such as silver, this leads to ferromagnetic behavior at $T<0$. In an fcc lattice, with an appreciable next nearest neighbor interaction, the situation is not so straightforward. It is possible that both the minimum ($T>0$) and maximum ($T<0$) energy states are antiferromagnetic. In this Letter, we report experiments on nuclear magnetism which show that rhodium is the first such metal found.

Rhodium has an fcc lattice and the metal consists 100% of the spin-$\frac{1}{2}$ isotope ^{103}Rh. In addition to the usual dipolar and Zeeman energies, the Hamiltonian H contains contributions from isotropic and anisotropic indirect exchange interactions [4,5]. We approximate the anisotropic part of the exchange by a pseudodipolar term and employ H in the form

$$H=H_{\rm dip}+H_{\rm pseudo}-\tfrac{1}{2}\sum_{ij}J_{ij}\mathbf{I}_i\cdot\mathbf{I}_j-\hbar\gamma\mathbf{B}\cdot\sum_i\mathbf{I}_i\,, \qquad (1)$$

where $\mathbf{B}$ is the external field and $\gamma/2\pi=1.34$ MHz/T is the gyromagnetic ratio, with $\mu=0.088\mu_N$. The terms $H_{\rm dip}$ and $H_{\rm pseudo}$ are of similar form and can be written as

$$H_{\rm dip}+H_{\rm pseudo}=\frac{1}{2}\sum_{i,j}\left\{\left(\frac{\mu_0\hbar^2\gamma^2}{4\pi r_{ij}^3}\right)+\tilde{B}_{ij}\right\}\times[\mathbf{I}_i\cdot\mathbf{I}_j-3(\mathbf{I}_i\cdot\hat{\mathbf{r}}_{ij})(\mathbf{I}_j\cdot\hat{\mathbf{r}}_{ij})]\,, \qquad (2)$$

where μ_0 is the permeability in vacuum and coefficients $\tilde{B}_{ij}$ are due to pseudodipolar interactions, whose magnitude can be deduced roughly from the measured NMR linewidths [6]; this yields for the nearest neighbor coefficients either $\tilde{B}_{nn}/h\approx1$ to 2 Hz or $\tilde{B}_{nn}/h\approx-18$ to -19 Hz.

We have investigated two Rh specimens with almost identical results. The first sample, made of 25-μm rhodium foil, contained about 100 ppm of iron which was responsible for the decrease of the Korringa constant from $\kappa=10$ sK to 0.06 sK in small magnetic fields; κ and the electronic temperature T_e determine the spin-lattice relaxation time $\tau_1=\kappa/T_e$. In this paper, we will mainly concentrate on the data obtained using our second specimen, which was a package of 28 foils with dimensions $4\times0.075\times25$ mm^3, oriented along the x, y, and z directions, respectively. The nominal purity of the material is 99.96+% and the total amount of magnetic impurities is less than 15 ppm; $\kappa=0.2$ sK in zero field. Preparation of the samples and their attachment to the first nuclear stage is described in Ref. [7]. Our samples were heat treated at 1300 °C in an oxygen atmosphere of 4×10^{-4} mbar for 16 h. This oxidized some of the iron impurities; employing the measured resistivities we estimate [7] 14 and 6 ppm for the effective iron content of our first and second samples, respectively.

The rhodium sample formed the second stage of our cascade nuclear demagnetization cryostat. The initial polarizations before demagnetization were limited by the long spin-lattice relaxation time of rhodium, $\tau_1=14$ h at 200 μK. Details of the cooling process and experimental techniques are described in Ref. [8]. Two Mumetal tubes, with a room-temperature shielding factor of 400, were installed to reduce the remnant field of the demagnetization magnet at the site of the sample. Measurements of longitudinal adiabatic susceptibility were employed to determine the residual field which varied between zero and 5 μT; typically it was below 2 μT. Strong supercooling [9], even after active compensation of the remnant field down to 0.2 μT, may have been the reason why we did not observe superconductivity below $T_c=325$ μK in our Rh samples.

To reach negative temperatures, the adiabatic demagnetization cooling of the specimen was stopped at a field of $B_{\rm inv}=0.4$ mT and a population inversion was per-

formed before continuing with the demagnetization. The inverted spin states were obtained by reversing B_{inv} quickly, in a time $\tau = 0.1$–1 ms, so that there was no chance for a redistribution of nuclei among the Zeeman energy levels within the spin-spin relaxation time $\tau_2 = 10.5$ ms. As in the case of silver the inversion efficiency depended strongly on polarization [2]. The best result, 95%, was reached for initial polarizations $p \leq 0.4$. The efficiency deteriorated very quickly with polarization, and the highest efficiency was 85% at $p = 0.7$ and only 60% at $p = 0.8$. Therefore, polarizations at $T < 0$ were limited to $p \cong -0.60$. Magnetic fields between 100 μT and 2 mT were tried but the inversion efficiency did not change appreciably.

The NMR spectra were recorded by using an rf SQUID while sweeping the frequency f of the excitation field. Several examples of the measured dynamic susceptibility in zero field, $\chi' - i\chi''$, both at $T > 0$ and $T < 0$, are displayed in Fig. 1. At negative temperatures $\chi'' < 0$, which is a signature of energy emission. The measured spectra agree quite well with the expression $\chi(f) = \chi_L(f) - \chi_L(-f)$, where χ_L is the usual Lorentzian line shape.

The static susceptibility $\chi'(0)$ can be calculated from $\chi''(f)$ by using the Kramers-Kronig equation $\chi'(0) = (2/\pi)\int_0^\infty [\chi''(f)/f]df$. The fitted curves of Fig. 1 were employed in the integration, actually performed between 0 and 150 Hz. To determine the susceptibility in absolute units, we utilized the fact that, at high fields ($B > 100$ μT), $\chi'(0)$ is proportional to the magnetization of the system [3], i.e., $1/\chi'(0) = B/\mu_0 p M_{sat} + N$ where M_{sat} is the saturation magnetization. The offset N, caused by demagnetization fields, was eliminated by a linear fit of $1/\chi'(0)$ vs $1/p$ over the range $p = 0.1$–0.7. Using the NMR frequency shifts in high fields, together with the dimensions of the samples, we estimate $D_x = 0.20$, $D_y = 0.75$, and $D_z = 0.05$.

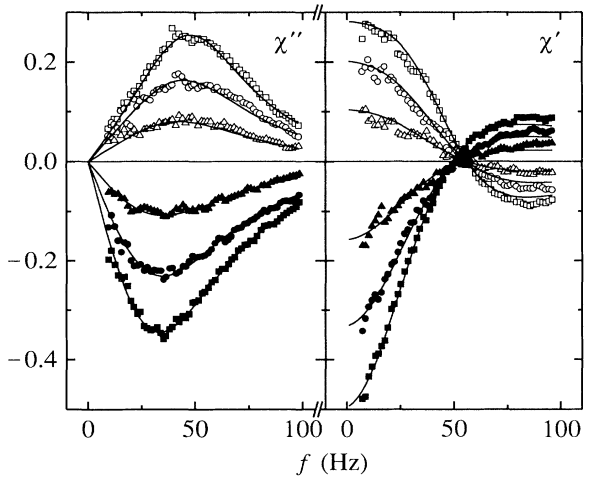

FIG. 1. NMR absorption χ'' and dispersion χ' curves of rhodium nuclei measured in zero magnetic field at initial polarizations $p = 0.51$ (□), 0.32 (○), and 0.15 (△) for $T > 0$, and $p = -0.51$ (■), -0.35 (●), and -0.17 (▲) for $T < 0$. The solid lines are least-squares fits of Lorentzian line shapes applied for the absorption and dispersion curves simultaneously (see text).

Additional NMR spectra, measured at 400 μT, were employed to calculate the polarization from the equation $p = \alpha\int\chi''(f)df$. The proportionality constant α was obtained from experiments around 1 mK, for which the initial polarization could be calculated from the temperature measured with pulsed NMR on platinum; the Pt scale, in turn, was calibrated against the superconducting transition point of Be.

The temperature of the Rh nuclei was determined using the second law of thermodynamics, $T = \Delta Q/\Delta S$, where ΔQ is the applied heat pulse to the spins and ΔS is the ensuing entropy change. The heat pulse was calculated according to $\Delta Q = \pi f \chi''(B_z^{rf})^2 \Delta t/\mu_0$, where $\Delta t = 2$–5 s is the duration of the rf excitation $B_z^{rf}\sin(2\pi f t)$; the homogeneity of the rf field was estimated to be better than 5%. The entropy was found from the polarization measured at 400 μT, using thermodynamic equations for the paramagnetic state. Our method applies to both positive and negative temperatures; at $T < 0$, $\Delta Q < 0$, i.e., the spins emit energy and $\chi'' < 0$ as seen in Fig. 1.

Since the rf excitation field was not well known owing to the Mumetal shields and other metallic parts surrounding the sample, B_z^{rf} was determined by adjusting the measured entropy to agree with the $1/T$ expansion at high temperatures: $S = (1/V_{mole})\mathcal{R}\ln 2 - (C/2\mu_0)(B_{loc}/T)^2$; here V_{mole} is the molar volume of Rh, $\mathcal{R}$ is the gas constant, and B_{loc} is the local field caused by the spin-spin interactions.

B_{loc} was carefully determined by measuring the field dependence of adiabatic susceptibility. According to theory [10], there is a relationship $\chi_\parallel \cong \chi_\perp/(1 + B^2/B_{loc}^2)$ between the longitudinal and transverse susceptibilities; this equation has proven reliable in calculating the local fields in copper and silver [8,11]. We applied it to our experimental data taken at $S/\mathcal{R}\ln 2 = 0.988$, with the assumptions that the Curie law $\chi_\perp = C/T$ is valid and that the field dependence of temperature can be determined by the isentropes $T^2 \propto B^2 + B_{loc}^2$. This yields for rhodium $B_{loc} = 34 \pm 3$ μT which is close to the value 35 μT measured in silver but much smaller than $B_{loc} = 0.36$ mT observed in copper.

Figure 2 displays the measured susceptibility as a function of polarization before demagnetization to zero field. At small polarizations, $\chi'(0)$ follows nicely the high-temperature approximation for susceptibility, viz.,

$$\chi'(0) = Ap/[1 - (R + L - D_z)Ap], \quad (3)$$

where $R = \sum_j J_{ij}/\mu_0 \rho \gamma^2 \hbar^2$, $L = \frac{1}{3}$ denotes the Lorentz factor due to long-range dipolar interactions, A is a constant, and ρ stands for the number density of rhodium atoms. This formula is obtained from the expression for static susceptibility according to the mean-field the-

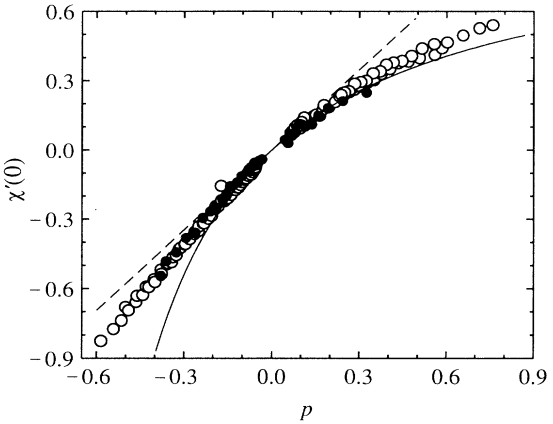

FIG. 2. Static susceptibility $\chi'(0)$ vs polarization p of rhodium nuclear spins measured in zero field for our first (●) and second (○) samples. The dashed line is the Curie susceptibility $\chi_0 = 1.16p$ and the solid curve depicts the mean-field behavior $\chi = \chi_0/[1 - \chi_0(R + L - D_z)]$, with $R = -1.35$.

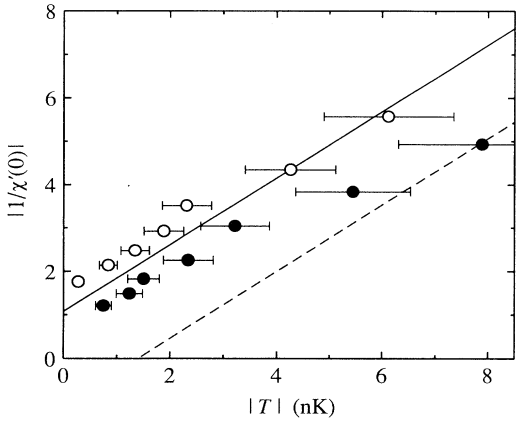

FIG. 3. Absolute value of the inverse static susceptibility $1/\chi'(0)$ of rhodium spins vs the absolute value of temperature measured at $T > 0$ (○) and at $T < 0$ (●). The solid line is the Curie-Weiss law with $\theta = -1.4$ nK, obtained from the low polarization data of Fig. 2 (see text); the dashed line is the corresponding ferromagnetic susceptibility for $T < 0$. The error bars depict the 20% uncertainty in the temperature measurement.

ory $\chi = \chi_0/[1 - (R + L - D)\chi_0]$, using $\chi_0 = (\mu_0 \mathcal{R} C/V_{\text{mole}} \times B_{\text{loc}}^2)^{1/2} p = Ap$ for the susceptibility of the noninteracting spin system; $C = 1.3$ nK for rhodium. Within the high-T approximation, $\chi_0 = Ap$ is equivalent to the Curie law $\chi_0 = C/T$.

The solid curve in Fig. 2 is a least-squares fit of Eq. (3), with $A = 1.16$, to the open circles in the range $-0.1 < p < 0.2$, yielding $R = -1.3 \pm 0.2$; the range of p in the fit was smaller at negative than at positive polarizations because deviations from the mean-field behavior are observed already when $p \leq -0.1$. If A is varied, too, we obtain $R = -1.4 \pm 0.1$ and $A = 1.29$. Hence, we conclude that $T = -1.35 \pm 0.2$ which is equivalent to $\sum_j J_{ij}/h = -146 \pm 22$ Hz as well as to $\theta = CR = -1.8 \pm 0.3$ nK for the Curie-Weiss parameter. This magnitude of R, intermediate between the values $R = 0.42$ and 2.5 for copper and silver, respectively, means that dipolar interactions may influence the ordered spin structures in rhodium substantially, although not as much as in copper [1].

At negative temperatures the susceptibility is a surprisingly linear function of polarization all the way down to $p = -0.6$. No saturation of $\chi'(0)$ was observed like in silver at $p_c = -0.49$, where ferromagnetic ordering set in [2].

The absolute value of $1/\chi'(0)$ is displayed in Fig. 3 as a function of $|T|$. The solid line is the antiferromagnetic Curie-Weiss law $\chi = C/(T - \theta_s)$, where we have employed $\theta_s = C(R + L - D_z) = -1.4$ nK obtained from the high-temperature analysis of the data in Fig. 2; at $T < 0$, this susceptibility corresponds to a ferromagnetic dependence displayed by the dashed line. At low temperatures, however, the Curie-Weiss approximation is known to deviate [12], especially in a spin-$\frac{1}{2}$ system, from the more accurate results based on high-T series expansions. When $T \approx |\theta|$, the inverse antiferromagnetic susceptibility, computed from series expansions [13], is about 20% larger than the value given by the Curie-Weiss law; this accounts for the small difference between the solid Curie-Weiss line in Fig. 3 and the data taken at $T > 0$.

At $T < 0$, the measured data display a crossover from ferromagnetic to antiferromagnetic behavior around -6 nK. This indicates that the energy of spins in rhodium is both minimized and maximized by antiferromagnetic order. The data at $T < 0$ extend to -750 pK which is roughly a factor of 2 closer to absolute zero than observed in the experiments on silver [2].

The ordered spin configurations, however, were not reached in rhodium. In particular, we searched meticulously for ordering at positive temperatures but no plateau in the $\chi(t)$ scans, characteristic of antiferromagnetic order, was observed in experiments at 0, 20, or 40 μT, up to initial polarizations of 83%. Compared with other systems [3], the ordering in rhodium is exceptionally hard to achieve; our starting condition is, i.e., about 6, 14, and 15 percentage units larger, respectively, than that required for antiferromagnetic ordering among silver nuclei [14].

From the expression for the local field [15],

$$B_{\text{loc}} = \left\{ B_{\text{dip}}^2 + S(S+1) \sum_j J_{ij}^2 / 2\hbar^2 \gamma^2 \right\}^{1/2},$$

we obtain $\sum_j J_{ij}^2/h^2 = 4086$ Hz^2. Here we have employed $B_{\text{dip}} = 17.4$ μT, which includes a 16% modification due to the estimated $\tilde{B}_{\text{nn}}$ coefficients. If we use the dipolar field, $B_{\text{dip}} = 15$ μT, computed from the magnetic moments alone, we obtain $\sum_j J_{ij}^2/h^2 = 4458$ Hz^2.

Combining the measured sums $\sum_j J_{ij}/h = -146$ Hz and $\sum_j J_{ij}^2/h^2 = 4086$ Hz^2, and assuming only nearest (J_{nn}) and next nearest neighbor (J_{nnn}) contributions,

we deduce two possible sets for interactions in rhodium: $\{J_{nn}/h = -17.1$ Hz, $J_{nnn}/h = 9.8$ Hz$\}$ or $\{J_{nn}/h = 0.9$ Hz, $J_{nnn}/h = -26.1$ Hz$\}$. The latter combination must be viewed with caution since such behavior of the J_{ij} coefficients would indicate that the next term, J_{nnnn}, should be included as well. The first set of J's looks reasonable although the decay of the interaction coefficients with distance is quite slow compared with similar estimates in silver [8] and the calculated behavior in copper and silver [5,16]. These sets for the interaction coefficients do not change much when $B_{dip} = 15$ μT is used in the analysis; we estimate ± 3 Hz for the accuracy of J's. Because of the complicated Fermi surface of rhodium, *ab initio* band structure calculations for the interaction coefficients are not available. We want to emphasize, however, that our first sample yielded almost the same values for the spin-spin interactions and, therefore, these results are not affected by the presence of magnetic impurities.

Molecular field calculations [17] have determined the ordered structures in the J_{nn}-J_{nnn} plane. Ferromagnetic ordering covers the region where both $J_{nn} > 0$ and $J_{nn} > -J_{nnn}$; the rest of the phase space is occupied by antiferromagnetic ordering. Our susceptibility results on Rh at $T < 0$, where effectively $J_{nn}^{T<0} = -J_{nn}^{T>0}$ and $J_{nnn}^{T<0} = -J_{nnn}^{T>0}$, indicate that the area covered by antiferromagnetic ordering is slightly larger than estimated by the molecular field theory. These interaction coefficients and the observed antiferromagnetic tendency mean that, according to this and more basic theories [18], the ordering in Rh takes place close to the phase boundaries of different magnetically ordered regions (type-I/type-III order at $T > 0$, and ferro/antiferromagnetic order at $T < 0$). In such a case, the transition temperatures are depressed substantially which could explain the absence of actual magnetic spin ordering in our experiments.

In summary, we have observed large differences in the integrated static susceptibility of Rh spins between $T > 0$ and $T < 0$. Antiferromagnetic susceptibility is found at positive temperatures while, at $T < 0$, the expected ferromagnetic behavior changes into a tendency towards antiferromagnetism. No ordered state was observed in these experiments even though the initial polarizations were as high as 83%; at $T < 0$, the polarization was limited to -60% owing to serious increases of entropy during the rapid field reversal. The minimum nuclear spin temperature measured in the paramagnetic state was 280 ± 60 pK which is a factor of 2 lower than the previous low-temperature record reached in silver.

We wish to acknowledge useful discussions with J. Kurkijärvi, O. V. Lounasmaa, M. T. Heinilä, and A. S. Oja. This work was financially supported by the Academy of Finland.

[1] See P. J. Hakonen, O. V. Lounasmaa, and A. S. Oja, J. Magn. Magn. Mater. **100**, 394 (1991), and references therein.
[2] P. J. Hakonen, K. K. Nummila, R. T. Vuorinen, and O. V. Lounasmaa, Phys. Rev. Lett. **68**, 365 (1992).
[3] See, e.g., A. Abragam and M. Goldman, *Nuclear Magnetism: Order and Disorder* (Clarendon, Oxford, 1982).
[4] A. S. Oja and P. Kumar, J. Low Temp. Phys. **66**, 155 (1987).
[5] A. S. Oja, X. W. Wang, and B. N. Harmon, Phys. Rev. B **39**, 4009 (1989).
[6] A. Narath, A. T. Fromhold, Jr., and E. D. Jones, Phys. Rev. **144**, 428 (1966).
[7] P. J. Hakonen, R. T. Vuorinen, and J. E. Martikainen (to be published).
[8] P. J. Hakonen and S. Yin, J. Low Temp. Phys. **85**, 25 (1991).
[9] Ch. Buchal, F. Pobell, R. M. Mueller, M. Kubota, J. R. Owers-Bradley, Phys. Rev. Lett. **50**, 64 (1983).
[10] See, e.g., A. G. Anderson, Phys. Rev. **125**, 1517 (1962), and references therein.
[11] G. J. Ehnholm, J. P. Ekström, J. F. Jacquinot, M. T. Loponen, O. V. Lounasmaa, and J. K. Soini, J. Low Temp. Phys. **39**, 417 (1980).
[12] See, e.g., L. J. de Jongh and A. R. Miedema, Adv. Phys. **23**, 1 (1974).
[13] M. T. Heinilä and A. S. Oja (private communication).
[14] P. J. Hakonen, S. Yin, and K. K. Nummila, Europhys. Lett. **15**, 677 (1991).
[15] R. P. Hudson, *Principles and Applications of Magnetic Cooling* (North-Holland, Amsterdam, 1972), p. 40.
[16] P.-A. Lindgård, X.-W. Wang, and B. N. Harmon, J. Magn. Magn. Mater. **54-57**, 1052 (1986); D. J. Miller and S. J. Frisken, J. Appl. Phys. **64**, 5630 (1988); B. N. Harmon, X.-W. Wang, and P.-A. Lindgård, J. Magn. Magn. Mater. **104-107**, 2113 (1992).
[17] See, e.g., J. S. Smart, *Effective Field Theories of Magnetism* (Saunders, Philadelphia, 1966).
[18] See, e.g., R. H. Swendsen, Phys. Rev. Lett. **32**, 1439 (1974).